Low-Complexity Delay-Doppler Channel Estimation in Discrete Zak Transform based OTFS

Vineetha Yogesh, Sandesh Rao Mattu, and A. Chockalingam

***Abstract*—In this letter, we propose a novel low-complexity delay Doppler (DD) channel estimation scheme suited for discrete Zak transform based orthogonal time frequency space (DZT-OTFS) systems with embedded pilot frame and fractional delays and Dopplers. Key novelties in the proposed scheme include i) decoupling the estimation of channel gains, delays, and Dopplers using a decoupled representation of the channel matrix that leads to low complexity, ii) use of the knowledge of the adjacent bin levels in the matched filter response of the transmit-receive pulses for delay estimation, and iii) de-rotating the phase introduced by channel delays/Dopplers to estimate channel gains. Simulation results show that the proposed estimation scheme achieves better normalized mean squared error and bit error performance at a lesser complexity compared to sparse Bayesian learning based estimation scheme in the literature.**

***Index Terms*—Discrete Zak transform, OTFS modulation, fractional delay-Doppler, DD channel estimation, embedded pilot.**

I. Introduction

Orthogonal time frequency space (OTFS) is a modulation scheme that mitigates the degrading effects of high Doppler spreads owing to its information multiplexing and signal processing in the delay-Doppler (DD) domain [1]. Most research on OTFS so far has primarily considered a two-step approach where information symbols multiplexed in the DD domain are first mapped to time-frequency domain which are then mapped to time domain for transmission, and vice versa at the receiver. Recently, a more promising single-step approach has emerged, where DD domain symbols are directly mapped to time domain for transmission (and vice versa at the receiver) using Zak transform [2]. This approach offers improved performance and reduced complexity compared to the two-step approach [3]- [6]. The recent work in [3], [4] has shown that Zak based OTFS is fundamentally different from two-step OTFS and that Zak based OTFS achieves better performance compared to the two-step OTFS over a larger range of delay and Doppler spreads. It also explains why Zak based OTFS is naturally suited to large doubly-spread channels and why it achieves better performance compared to TDM, FDM, and two-step OTFS. In a related work, the authors in [5] have considered a discrete Zak transform (DZT) based OTFS system, referred to as DZT-OTFS, and derived its input-output relation. The bit error performance of this DZT-OTFS system has been studied in [6] assuming perfect channel knowledge, where it has been shown that DZT-OTFS performs better than two-step OTFS. In this letter, we consider the problem of DD channel estimation for DZT-OTFS systems with embedded pilot frame and fractional delay-Dopplers. Specifically, we propose a novel low-complexity DD channel estimation scheme for DZT-OTFS.

In the proposed algorithm, we decouple the channel matrix into contributions of delay, Doppler, and the channel coefficient for the purpose of channel estimation. This forms the first key novelty[1]. The way this decoupling is exploited constitutes other two key novelties, as follows. An initial fine estimation of delay, independent of Doppler and channel coefficient is obtained by exploiting the matched filter characteristics and the channel interaction by defining a normalized adjacent bin level vector. This is the second novelty. The third novelty is the modeling of channel coefficient as a function of delay and Doppler and de-rotating the phase introduced by the channel spreads. The second and third novelties result in a reduced complexity 1D search for Doppler and delay, rather than a more complex joint 2D search. Simulation results show that all the above novelties result in a low-complexity algorithm with good performance. The performance of the proposed algorithm is compared with that of the off-grid sparse Bayesian learning (SBL) based channel estimation algorithm in [9]. Results show that the proposed algorithm performs better than SBL, while also being more computationally efficient.

II. DZT-OTFS system model

At the DZT-OTFS transmitter, $N = KL$ information symbols from a modulation alphabet $\mathbb{A}$, denoted by $\mathbf{Z}_{\mathbf{x}}[k,l]$s, are multiplexed over a $K \times L$ DD grid given by $\left\{\left(k\Delta\nu = \frac{k}{KLT_{\rm s}}, l\Delta\tau = lT_{\rm s}\right),\ k = 0, \cdots, K-1,\ l = 0, \cdots, L-1\right\}$, where $T_{\rm s} = 1/B$ is the symbol duration, B is the bandwidth available for communication, and $\Delta\tau$ and $\Delta\nu$ are the delay and Doppler resolutions, respectively. The DD domain symbols, $\mathbf{Z}_{\mathbf{x}}[k,l]$s, are converted to time domain (TD) using inverse discrete Zak transform (IDZT) [5], [10], as

$$\mathbf{x}[n] = \frac{1}{\sqrt{K}} \sum_{k=0}^{K-1} \mathbf{Z}_{\mathbf{x}}[k, (n)_L] e^{j2\pi \frac{\lfloor n/L \rfloor}{K} k}, \tag{1}$$

where $(\cdot)_L$ denotes modulo-L operation and $\lfloor \cdot \rfloor$ denotes floor operation. To mitigate inter-frame interference, a cyclic prefix of length $N_{\rm cp}$ is added in the TD. The TD sequence is mounted on time-shifted transmit pulse $p_{\rm tx}(t), 0 \le t \le T_{\rm s}$, resulting in a continuous time signal $x_{\rm t}(t)$, given by

Manuscript submitted October 10, 2023; revised December 13, 2023; accepted December 31, 2023. This work was supported in part by the J. C. Bose National Fellowship, Department of Science and Technology, Government of India. The first author would like to thank the Prime Minister's Research Fellowship, Ministry of Education, Government of India for the support. The associate editor coordinating the review of this paper and approving it for publication was Dr. Weijie Yuan (*Corresponding author: A. Chockalingam)*. The authors are with the Department of ECE, Indian Institute of Science, Bangalore, Karnataka, India, 560012. E-mail: {vineethay; sandeshmattu; achockal}@iisc.ac.in.

[1]The work in [7] also uses a decoupling of the effective channel matrix, which is different from ours as follows. First, [7] does the decoupling for a two-step OTFS system, whereas we do it for a DZT-OTFS system. Second, the decoupling in [7] leaves out a residual term which is both delay and Doppler dependent (see the term $\mathcal{L}_{l,k}(\nu_i)$ in [7, Eqn. (4)]), making the decoupling as approximate. Whereas, in our decoupling in this letter, there is no such residual term. Also, while [7] considers a rectangular pulse, our work considers general pulse shapes.

$$x_{\rm t}(t) = \sum_{n=0}^{N+N_{\rm cp}-1} \mathbf{x}[(n-N_{\rm cp})_N] p_{\rm tx}(t-nT_{\rm s}), \quad (2)$$

where $0 \le t \le (N+N_{\rm cp})T_{\rm s}$. The transmitted signal $x_{\rm t}(t)$ passes through a doubly-spread channel having maximum delay and Doppler spreads, denoted by $\tau_{\max}$ and $\nu_{\max}$, respectively. The DD domain response is given by $h(\tau,\nu) = \sum_{i=1}^{P} h_i \delta(\tau-\tau_i)\delta(\nu-\nu_i)$, where P is the number of paths in the DD domain. For the ith path, h_i is the channel coefficient, $\tau_i = \alpha_i T_{\rm s}$ is the delay, where $\alpha_i = L_i + l_i$ with L_i being the integer part and $l_i \in (-0.5, 0.5]$ being the fractional part, and $\nu_i = \frac{\beta_i}{KLT_{\rm s}}$ is the Doppler, where $\beta_i = K_i + k_i$ with K_i being the integer part and $k_i \in (-0.5, 0.5]$ being the fractional part, such that $\tau_i \in [0, \tau_{\max}]$ and $\nu_i \in [-\nu_{\max}, \nu_{\max}]$. The received TD signal $r(t)$ at the receiver is given by

$$r(t) = \int_{\nu}\int_{\tau} h(\tau,\nu) x_{\rm t}(t-\tau) e^{j2\pi\nu(t-\tau)} d\tau d\nu + w(t), \quad (3)$$

where $w(t)$ is the additive noise at the receiver. Matched filtering (MF) is performed at the receiver by choosing receive pulse $p_{\rm rx}(t) = p_{\rm tx}(t) = p(t)$ and assuming $B \gg \nu_{\max}$. The output is sampled at $t = mT_{\rm s}, m = 0, 1, \cdots, N+N_{\rm cp}-1$. After discarding the first $N_{\rm cp}$ samples, the discrete TD signal obtained is [5]

$$\mathbf{y}[m] = \sum_{i=1}^{P} h_i \sum_{n=0}^{N-1} \mathbf{x}[n]\mathbf{g}[(m-n)T_{\rm s} - \tau_i] e^{j2\pi\nu_i(\tau_i + nT_{\rm s})} + \mathbf{v}[m], \quad (4)$$

where $g(t) \triangleq \int_{\tau} p(\tau) p^*(t-\tau) d\tau$ is the effective pulse at the output of MF, $\mathbf{g}[m]$ and $\mathbf{v}[m]$ are samples of MF response and MF noise, respectively. Simplifying (4) by substituting for τ_i and ν_i, we get the received vector $\mathbf{y} \in \mathbb{C}^{1\times N}$ as

$$\mathbf{y}[m] = \sum_{i=1}^{P} h_i e^{\frac{j2\pi\alpha_i\beta_i}{N}} \sum_{n=0}^{N-1} \mathbf{x}[n]\mathbf{e}_i[n]\mathbf{g}_i[m-n] + \mathbf{v}[m] \quad (5)$$

$$= \sum_{i=1}^{P} h_i' \mathbf{y}_i[m] + \mathbf{v}[m], \quad (6)$$

where $h_i' = h_i e^{\frac{j2\pi\alpha_i\beta_i}{N}}$, $\mathbf{g}_i[n] = \mathbf{g}[n-\alpha_i]$, $\mathbf{e}_i[n] = e^{j2\pi\frac{\beta_i}{N}n}$, and $m, n = 0, \cdots, N-1$. Here, $\mathbf{g}_i[n]$ and $\mathbf{e}_i[n]$ are the discrete sequences that capture the effect of delay and Doppler of the ith path, respectively, and $\mathbf{y}_i[m]$ is the component of received signal corresponding to the ith path, given by

$$\mathbf{y}_i[m] = \sum_{n=0}^{N-1} \mathbf{x}[n]\mathbf{e}_i[n]\mathbf{g}_i[m-n]. \quad (7)$$

At the receiver, $\mathbf{y}$ is converted to DD domain using DZT as

$$\mathbf{Z}_{\mathbf{y}}[k,l] = \frac{1}{\sqrt{K}} \sum_{n=0}^{K-1} \mathbf{y}[l+nL] e^{-j2\pi\frac{k}{K}n}. \quad (8)$$

The equivalent DD domain representations of (6) and (7) are

$$\mathbf{Z}_{\mathbf{y}}[k,l] = \sum_{i=1}^{P} h_i' \mathbf{Z}_{\mathbf{y}_i}[k,l] + \mathbf{Z}_{\mathbf{v}}[k,l], \quad (9)$$

$$\mathbf{Z}_{\mathbf{y}_i}[k,l] = \sum_{m=0}^{L-1}\sum_{n=0}^{K-1} \mathbf{Z}_{\mathbf{x}}[n,m]\mathbf{Z}_{\mathbf{e}_i}[k-n,m]\mathbf{Z}_{\mathbf{g}_i}[k,l-m], \quad (10)$$

respectively, where $\mathbf{Z}_{\mathbf{e}_i}$, $\mathbf{Z}_{\mathbf{g}_i}$, and $\mathbf{Z}_{\mathbf{v}}$ are the DZT of the sequences $\mathbf{e}_i$, $\mathbf{g}_i$, and $\mathbf{v}$, respectively.

Further, for vectorizing (9), let $\mathbf{B}_u$ be a $K \times K$ matrix whose jth row is $\mathbf{B}_u[j-1,:] = (\mathbf{Z}_{\mathbf{e}_i}[:, u-1])^T \mathbf{P}_K^{j-1}$, where $u = 1, \cdots, L$, $j = 1, \cdots, K$, and $\mathbf{P}_K$ is a $K \times K$ basic circulant permutation matrix (BCPM) [8]. Next, define block diagonal matrix $\mathbf{E}_i$ with matrices $\{\mathbf{B}_u\}_{u=1}^{L}$ along the diagonal. Likewise, define a $K \times N$ block matrix $\mathbf{A} = [\text{diag}\{\mathbf{Z}_{\mathbf{g}_i}[:,0]\}, \cdots, \text{diag}\{\mathbf{Z}_{\mathbf{g}_i}[:,L-1]\}]$. Let $\mathbf{Q}_u = \mathbf{P}_L^{u-1} \otimes \mathbf{I}_K$ be an $N \times N$ matrix, where $\mathbf{P}_L$ is an $L \times L$ BCPM and $\otimes$ operator denotes Kronecker product. Also, define an $N \times N$ matrix $\mathbf{G}_i = \begin{bmatrix} \mathbf{A}\mathbf{Q}_1 \\ \vdots \\ \mathbf{A}\mathbf{Q}_L \end{bmatrix}$. Using $\mathbf{E}_i$ and $\mathbf{G}_i$, the effective channel matrix $\mathbf{H}$ in DD domain can be written as

$$\mathbf{H} = \sum_{i=1}^{P} h_i' \mathbf{E}_i \mathbf{G}_i. \quad (11)$$

Note that, since $\mathbf{G}_i$s capture the effect of delays (α_is) and $\mathbf{E}_i$s capture the effect of Dopplers (β_is), the channel representation in (11) is in a form that decouples the effect of channel gains (h_is), delays (α_is), and Dopplers (β_is). This decoupled representation is instrumental in devising the low complexity algorithm proposed in Sec. III. Finally, (9) can be written as

$$\mathbf{y}_{\rm DD} = \mathbf{x}_{\rm DD}\mathbf{H} + \mathbf{v}_{\rm DD}, \quad (12)$$

where $\mathbf{y}_{\rm DD}, \mathbf{x}_{\rm DD}, \mathbf{v}_{\rm DD} \in \mathbb{C}^{1\times N}$ are vectorized column-wise, such that $\mathbf{y}_{\rm DD}[k+Kl] = \mathbf{Z}_{\mathbf{y}}[k,l]$, $\mathbf{x}_{\rm DD}[k+Kl] = \mathbf{Z}_{\mathbf{x}}[k,l]$, and $\mathbf{v}_{\rm DD}[k+Kl] = \mathbf{Z}_{\mathbf{v}}[k,l]$.

At the receiver, an estimate of the effective channel matrix $\mathbf{H}$ is needed for the detection of data symbols. For this, we consider embedded pilot frames, where each frame consists of a pilot symbol, guard symbols, and data symbols, defined by

$$\mathbf{X}_{\rm pd}[k,l] = \begin{cases} \sqrt{E_{\rm p}} & \text{for } k = k_{\rm tx}, l = l_{\rm tx}, \\ 0 & \text{for } k \in k_{\rm ind}, l \in l_{\rm ind}, \\ a\sqrt{E_{\rm d}} & \text{otherwise}, \end{cases} \quad (13)$$

where $(k_{\rm tx}, l_{\rm tx})$ is the pilot location in the frame, $k_{\rm ind}$ and $l_{\rm ind}$ defined by the closed intervals $[k_{\rm tx}-2K_{\max}, k_{\rm tx}+2K_{\max}]$ and $[l_{\rm tx}-L_{\max}, l_{\rm tx}+L_{\max}]$, respectively, excluding $k_{\rm tx}$ in $k_{\rm ind}$ and $l_{\rm tx}$ in $l_{\rm ind}$, denote the guard space around the pilot to mitigate the interference between pilot and data symbols[2], $K_{\max} = \lceil \nu_{\max}/\Delta\nu \rceil$, $L_{\max} = \lceil \tau_{\max}/\Delta\tau \rceil$, $E_{\rm p} = \sigma_{\rm p}^2 KL$ is the energy of the pilot, $E_{\rm d} = \sigma_{\rm d}^2 KL/N_{\rm d}$ is the average energy in data, where $\lceil\cdot\rceil$ denotes the ceil operation, $a \in \mathbb{A}$, and $\sigma_{\rm p}^2 + \sigma_{\rm d}^2 = E_{\rm f}$, the average frame energy. The number of bins used for channel estimation (pilot and guard) is $N_{\rm p} = (4K_{\max}+1)(2L_{\max}+1)$ and $N_{\rm p} + N_{\rm d} = KL$, $N_{\rm d}$ is the number of bins used for data.

At the receiver, $\mathbf{Z}'_{\mathbf{y}} = \mathbf{Z}_{\mathbf{y}} \odot \mathbf{M}$ is used for channel estimation, where $\mathbf{M} \in \{0,1\}^{K\times L}$ such that

$$\mathbf{M}[k,l] = \begin{cases} 1 & \text{for } k \in \mathcal{K}, l \in \mathcal{L}, \\ 0 & \text{otherwise}, \end{cases} \quad (14)$$

[2]In case of integer DDs, the channel response is better localized and hence the guard space is adequate to limit the interference between pilot and data. However, in case of fractional DDs, the channel response gets spread beyond the guard space causing pilot and data interfering with each other, thus influencing the channel estimation and data detection performance. We consider fractional DDs in this letter.

where $\mathcal{K} = \{k_{\rm tx} - K_{\max}, k_{\rm tx} - K_{\max} + 1, \cdots, k_{\rm tx} + K_{\max}\}$, $\mathcal{L} = \{l_{\rm tx}, l_{\rm tx}+1, \cdots, l_{\rm tx}+L_{\max}\}$, and $\odot$ is Hadamard product.

III. Proposed Channel Estimation Algorithm

The algorithm is proposed for fractional DDs. No knowledge of the number of paths is assumed. The nature of the channel spread may be such that two or more paths overlap significantly. Therefore, the proposed algorithm estimates $P' \geq P$ paths with $P' \leq P_{\max}$, where $P_{\max}$ is the maximum number of paths estimated after which the algorithm terminates. In the proposed algorithm, the 3-tuple estimation problem is reduced to a 2-tuple estimation problem, by modeling h_i in terms of α_i and βi as follows.

For the ith path, the location of the maximum energy bin in the frame $\mathbf{Z}'^{(i)}_{\mathbf{y}}$ (see Sec. III-C) is $(k^{(i)}_{\rm rx}, l^{(i)}_{\rm rx})$. From (11), we note that the conventional way of obtaining channel coefficient vector $\mathbf{h} = [h'_1 \;\; h'_2 \;\; \cdots \;\; h'_P]$ from the received pilot vector $\mathbf{y}_{\rm DD}$ provides erroneous estimate due to the phase rotation introduced by the channel path delay and Doppler components. Hence, to obtain a true estimate of $\mathbf{h}$, it is necessary to de-rotate the received pilot symbol through construction of $\mathbf{\Phi}_{\hat{\alpha}_i,\hat{\beta}_i} = \mathbf{x}_{\rm p}\hat{\mathbf{E}}_i(\hat{\beta}_i)\hat{\mathbf{G}}_i(\hat{\alpha}_i)$, with $\hat{\mathbf{G}}_i(\hat{\alpha}_i)$ and $\hat{\mathbf{E}}_i(\hat{\beta}_i)$ computed by using the estimated delay and Doppler indices $\hat{\alpha}_i$ and $\hat{\beta}_i$ in $\mathbf{G}_i$ and $\mathbf{E}_i$, respectively, as described in Sec. II, and $\mathbf{x}_{\rm p}[k + Kl] = \mathbf{X}_{\rm pd}[k, l]$, with $a = 0$ (only pilot symbol). The estimate of the channel coefficient for the ith path, $\hat{h}_i$, can then be obtained as

$$\hat{h}_i(\hat{\alpha}_i, \hat{\beta}_i) = \frac{\mathbf{Z}'^{(i)}_{\mathbf{y}}[k^{(i)}_{\rm rx},\; l^{(i)}_{\rm rx}]}{\mathbf{\Phi}_{\hat{\alpha}_i,\hat{\beta}_i}[Kl^{(i)}_{\rm rx} + k^{(i)}_{\rm rx}]}. \tag{15}$$

Further, we take advantage of the decoupled nature of h'_is (channel coefficients), $\mathbf{E}_i$ matrices (Dopplers), and $\mathbf{G}_i$ matrices (delays) in the expression for the $\mathbf{H}$ matrix in (11) to develop sub-algorithms to separately estimate channel delays and Dopplers. This results in a decoupled low-complexity 1D search for delay and Doppler, as opposed to a high-complexity joint 2D search. To begin, the algorithm obtains coarse estimates of the channel parameters. Later, these estimates are refined. The refinement stages are proposed based on the channel interaction with pilot symbols along the delay and Doppler axes. Further, the role of the effective transmit and receive pulse $g(t)$ is considered in the refinement stage. Figure 1 illustrates the flowchart of the proposed algorithm, where a color coding is used in blocks to indicate the three steps involved. Red blocks correspond to operations carried out in Step 1, blue blocks correspond to operations in Step 2, and yellow blocks correspond to operations in Step 3. The descriptions of the three steps are provided below.

A. *Step 1*: Coarse estimate ($\hat{\alpha}^{(c)}, \hat{\beta}^{(c)}$)

The coarse estimates of the delay and Doppler indices of ith path, denoted by $\hat{\alpha}^{(c)}_i$ and $\hat{\beta}^{(c)}_i$, respectively, are obtained based on the observation that, due to ith path delay and Doppler, the received pilot energy is concentrated around $(k^{(i)}_{\rm rx}, l^{(i)}_{\rm rx})$, i.e., the location in the received pilot frame corresponding to the delay and Doppler of the corresponding path. For ith path, the delay-Doppler indices tuple is obtained as

$$(k^{(i)}_{\rm rx}, l^{(i)}_{\rm rx}) = \arg\max_{k,l} \left|\mathbf{Z}'^{(i)}_{\mathbf{y}}[k, l]\right|^2, \tag{16}$$

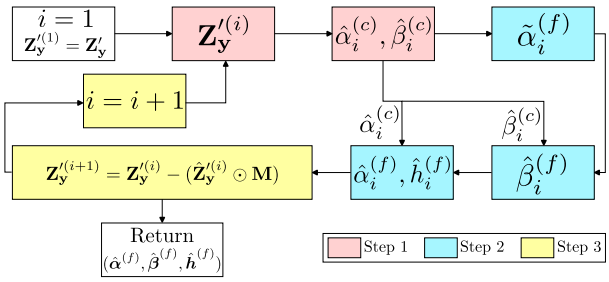

Fig. 1. Proposed DD channel estimation algorithm flowchart.

Algorithm 1 Fractional estimation of ith path delay

Inputs: $\breve{\mathbf{Z}}^{(i)}_{\mathbf{y}} = |\mathbf{Z}'^{(i)}_{\mathbf{y}}|$, indices $(k^{(i)}_{\rm rx}, l^{(i)}_{\rm rx})$ given by (16), coarse estimate $\hat{\alpha}^{(c)}_i$, resolution Δ_α

Initialize: Search range $\mathcal{J} = \{\hat{\alpha}^{(c)}_i - 0.5, \hat{\alpha}^{(c)}_i - 0.5 + \Delta_\alpha, \hat{\alpha}^{(c)}_i - 0.5 + 2\Delta_\alpha, \; \cdots, \; \hat{\alpha}^{(c)}_i + 0.5\}$,
$\mathbf{z}^{(i)}_{\rm NABL} = \frac{[\breve{\mathbf{Z}}^{(i)}_{\mathbf{y}}[k^{(i)}_{\rm rx}, l^{(i)}_{\rm rx}-q] \;\; \breve{\mathbf{Z}}^{(i)}_{\mathbf{y}}[k^{(i)}_{\rm rx}, l^{(i)}_{\rm rx}-q+1] \cdots \breve{\mathbf{Z}}^{(i)}_{\mathbf{y}}[k^{(i)}_{\rm rx}, l^{(i)}_{\rm rx}+q]]}{\breve{\mathbf{Z}}^{(i)}_{\mathbf{y}}[k^{(i)}_{\rm rx}, l^{(i)}_{\rm rx}]}$,
$J = \overline{\overline{\mathcal{J}}}$, where $\bar{\cdot}$ denotes cardinality of a set, $j = 1$

Define: $\mathbf{g}[n; d]$ as the sampled version of $g(t)$, with the samples delayed by d, $\breve{\mathbf{g}}[n; d] = |\mathbf{g}[n; d]|$

repeat

  Compute $\breve{\mathbf{g}}[n; \mathcal{J}(j)]$

  $m = \arg\max^{n} \breve{\mathbf{g}}[n; \mathcal{J}(j)]$

  $\mathbf{g}_{\rm NABL}(\mathcal{J}(j)) = \frac{[\breve{\mathbf{g}}[m-q; \mathcal{J}(j)] \;\; \breve{\mathbf{g}}[m-q+1; \mathcal{J}(j)] \cdots \breve{\mathbf{g}}[m+q; \mathcal{J}(j)]]}{\breve{\mathbf{g}}[m; \mathcal{J}(j)]}$

  update $j = j + 1$

until $j = J$

Output: $\tilde{\alpha}^{(f)}_i = \arg\min_{\mathcal{J}(j)} \|\mathbf{z}^{(i)}_{\rm NABL} - \mathbf{g}_{\rm NABL}(\mathcal{J}(j))\|_1$

where $|\cdot|$ denotes the absolute value. The coarse estimates of the path delay $\hat{\alpha}^{(c)}_i$ and the path Doppler $\hat{\beta}^{(c)}_i$ are obtained as

$$\hat{\alpha}^{(c)}_i = l^{(i)}_{\rm rx} - l_{\rm tx}, \quad \hat{\beta}^{(c)}_i = k^{(i)}_{\rm rx} - k_{\rm tx}. \tag{17}$$

B. *Step 2*: Fine estimate ($\hat{\alpha}^{(f)}$,$\hat{\beta}^{(f)}$,$\hat{h}^{(f)}$)

A naive approach for fine estimation is a brute-force search over the DD grid surrounding the coarse estimates. However, this leads to high complexity. Therefore, fine estimation is carried out differently by taking advantage of the knowledge of the MF response characteristics of the transmit-receive pulses. First, a fractional estimate of delay $\tilde{\alpha}^{(f)}_i$ is obtained using this knowledge. This estimated $\tilde{\alpha}^{(f)}_i$ is then used to obtain a fine estimate of Doppler $\hat{\beta}^{(f)}_i$, which, in turn, is used to obtain a fine estimate of delay $\hat{\alpha}^{(f)}_i$.

The procedure for estimating $\tilde{\alpha}^{(f)}$ is listed in **Algorithm 1**. The intuition behind **Algorithm 1** is as follows (being a heuristic, a formal performance analysis is quite involved which can be taken up for future work). The received signal's spread along delay axis in the DD domain (after interaction with channel and matched filtering) has a similar shape as that of $g(t)$, the effective transmit-receive pulse after MF operation. We look for that delay which results in maximum similarity between received vector $\mathbf{Z}'_{\mathbf{y}}$ and the MF response vector $\mathbf{g}$, the discrete version of $g(t)$. We do this by minimizing the L1-norm between $\mathbf{Z}'_{\mathbf{y}}$ and delayed versions of $\mathbf{g}$ over delays around the coarse estimate $\hat{\alpha}^{(c)}$ as follows.

For the ith path, we minimize the L1-norm between the normalized received vector and the MF response vector of lengths $2q+1$ centered around their respective maximum amplitude locations, where q is the number of bins on either side of the maximum amplitude location. We refer to these $(2q+1)$-length vectors as the *normalized adjacent bin level (NABL) vectors*. The received NABL vector is denoted by $\mathbf{z}^{(i)}_{\text{NABL}}$ (see step 2 of **Algorithm 1**). The MF response NABL vector, denoted by $\mathbf{g}_{\text{NABL}}$, is obtained as follows. The delays around $\hat{\alpha}_i^{(c)}$ for fine search is defined as $\mathcal{J} = \{\hat{\alpha}_i^{(c)} - 0.5, \hat{\alpha}_i^{(c)} - 0.5 + \Delta_\alpha, \hat{\alpha}_i^{(c)} - 0.5 + 2\Delta_\alpha, \cdots, \hat{\alpha}_i^{(c)} + 0.5\}$, where Δ_α is the delay search resolution. For each $\mathcal{J}(j)$, $g(t;\mathcal{J}(j))$ is obtained by delaying $g(t)$ by $\mathcal{J}(j)T_{\text{s}}$, which on sampling at T_{s} intervals (i.e., $t = nT_{\text{s}}$) yields $\mathbf{g}[n;\mathcal{J}(j)]$, where $n = 0, 1, \cdots, N-1$. Now, for each $\mathbf{g}[n;\mathcal{J}(j)]$, the location of maximum amplitude is obtained as $m = \arg\max_n \breve{\mathbf{g}}[n;\mathcal{J}(j)]$ (see step 6). Next, the $\mathbf{g}_{\text{NABL}}(\mathcal{J}(j))$ vector is obtained by picking q values on either side of m (see step 7). Finally, a minimization of $\|\mathbf{z}^{(i)}_{\text{NABL}} - \mathbf{g}_{\text{NABL}}(\mathcal{J}(j))\|_1$ is performed over $\mathcal{J}(j)$ to obtain $\tilde{\alpha}_i^{(f)}$ (see step 10). We have carried out simulations for different values of q and observed that $q = 1$ attains the best normalized mean square error (NMSE) and bit error rate (BER) performance. We also observed through simulations that L1-norm gives more robust estimation compared to L2-norm. Hence, we adopt $q = 1$ and L1-norm in all the simulations.

The estimated $\tilde{\alpha}_i^{(f)}$ is then used to obtain $\hat{\beta}_i^{(f)}$ as follows. The fine Doppler search area is defined as $\mathcal{G} = \{\hat{\beta}_i^{(c)} - 0.5, \hat{\beta}_i^{(c)} - 0.5 + \Delta_\beta, \hat{\beta}_i^{(c)} - 0.5 + 2\Delta_\beta, \cdots, \hat{\beta}_i^{(c)} + 0.5\}$, where Δ_β is the Doppler search resolution. For each $\zeta_m \in \mathcal{G}$, $m = 1, 2, \cdots, \overline{\overline{\mathcal{G}}}$, the channel coefficients $(h_i^{(c)}(\zeta_m))$ are computed using (15) (with $\hat{\alpha}_i = \tilde{\alpha}_i^{(f)}$, $\hat{\beta}_i = \zeta_m$), followed by the computation of the channel matrix, $\hat{\mathbf{H}}(\tilde{\alpha}_i^{(f)}, \zeta_m, h_i^{(c)}(\zeta_m))$ using (11). Now, we define $\mathbf{z}_{\mathbf{y}}^{\prime(i)} \in \mathbb{C}^{1\times N}$ such that $\mathbf{z}_{\mathbf{y}}^{\prime(i)}[k + Kl] = \mathbf{Z}_{\mathbf{y}}^{\prime(i)}[k,l]$. A maximum likelihood (ML) estimate of Doppler is obtained by maximizing the log-likelihood function over $\mathcal{G}$, i.e., $\arg\max_{\zeta_m \in \mathcal{G}} \log(P(\mathbf{Z}_{\mathbf{y}}^{(i)} | \hat{\mathbf{H}}(\tilde{\alpha}_i^{(f)}, \zeta_m, h_i^{(c)}(\zeta_m)), \mathbf{x}_{\text{p}}))$, which is equivalent to

$$\hat{\beta}_i^{(f)} = \arg\min_{\zeta_m \in \mathcal{G}} \left\| \mathbf{z}_{\mathbf{y}}^{\prime(i)} - \mathbf{x}_{\text{p}} \hat{\mathbf{H}}(\tilde{\alpha}_i^{(f)}, \zeta_m, h_i^{(c)}(\zeta_m)) \right\|_2, \quad (18)$$

where $P(\mathbf{Z}_{\mathbf{y}}^{(i)} | \hat{\mathbf{H}}, \mathbf{x}_{\text{p}}) \sim \mathcal{CN}(\mathbf{x}_{\text{p}}\hat{\mathbf{H}}, \sigma^2\mathbf{I})$, $\sigma^2\mathbf{I}$ is the $N \times N$ covariance matrix of noise ($\mathbf{v}_{\text{DD}}$), and $\|\cdot\|_2$ is vector 2-norm.

This $\hat{\beta}_i^{(f)}$ is used to obtain a refined delay estimate $\hat{\alpha}_i^{(f)}$. Following similar procedure as described above, an ML estimate of delay is obtained in (19), where the search is carried over $\mu_m \in \mathcal{J}$, for $m = 1, 2, \cdots, \overline{\overline{\mathcal{J}}}$. For each μ_m, the channel coefficients $h_i^{(c)}(\mu_m)$ are computed using (15) (with $\hat{\alpha}_i = \mu_m$, $\hat{\beta}_i = \hat{\beta}_i^{(f)}$), followed by the computation of the channel matrix, $\hat{\mathbf{H}}(\mu_m, \hat{\beta}_i^{(f)}, h_i^{(c)}(\mu_m))$, and $\hat{\alpha}_i^{(f)}$ is obtained as

$$\hat{\alpha}_i^{(f)} = \arg\min_{\mu_m \in \mathcal{J}} \left\| \mathbf{z}_{\mathbf{y}}^{\prime(i)} - \mathbf{x}_{\text{p}} \hat{\mathbf{H}}(\mu_m, \hat{\beta}_i^{(f)}, h_i^{(c)}(\mu_m)) \right\|_2. \quad (19)$$

The fine estimate of channel coefficient $\hat{h}_i^{(f)}$ is obtained using (15). We note that while $\tilde{\alpha}_i^{(f)}$ is an initial estimate, $\hat{\alpha}_i^{(f)}$ is a refined estimate, refined using the knowledge of $\hat{\beta}_i^{(f)}$ and $h_i^{(c)}$ in (19), and the refinement helps to improve performance.

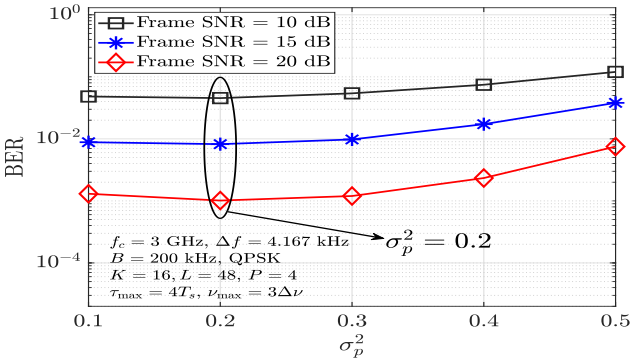

Fig. 2. BER performance for proposed as a function of σ_{p}^2.

C. *Step 3*: *Inter-path interference cancellation*

Recall that, due to fractional nature of the DD channel, the effect of one path may interfere with that of another, leading to inaccurate estimates. The estimation can be performed without cancelling this interference, using Steps 1 and 2 described above. However, this leads to poor performance. Hence, in the proposed algorithm, once the ith path parameters are estimated, the effect of this estimated path is removed from $\mathbf{Z}_{\mathbf{y}}^{\prime(i)}$. To do this, the channel matrix for the ith path, $\hat{\mathbf{H}}(\hat{\alpha}_i^{(f)}, \hat{\beta}_i^{(f)}, \hat{h}_i^{(f)})$, is constructed using which we define $\hat{\mathbf{z}}_{\mathbf{y}}^{\prime(i)} = \mathbf{x}_{\text{p}}\hat{\mathbf{H}}(\hat{\alpha}_i^{(f)}, \hat{\beta}_i^{(f)}, \hat{h}_i^{(f)})$. Next, $\hat{\mathbf{Z}}_{\mathbf{y}}^{\prime(i)} \in \mathbb{C}^{K\times L}$ such that $\hat{\mathbf{Z}}_{\mathbf{y}}^{\prime(i)}[k,l] = \hat{\mathbf{z}}_{\mathbf{y}}^{\prime(i)}[k + Kl]$ is used for cancellation as

$$\mathbf{Z}_{\mathbf{y}}^{\prime(i+1)} = \mathbf{Z}_{\mathbf{y}}^{\prime(i)} - (\hat{\mathbf{Z}}_{\mathbf{y}}^{\prime(i)} \odot \mathbf{M}), \quad (20)$$

and $\mathbf{Z}_{\mathbf{y}}^{\prime(i+1)}$ is taken as the received pilot frame to estimate the channel parameters for the $(i+1)$th path.

Stopping criterion: The algorithm stops at the ith iteration if either $i = P_{\max}$ or $\left| \|\mathbf{Z}_{\mathbf{y}}^{\prime(i)}\|_F - \|\mathbf{Z}_{\mathbf{y}}^{\prime(i-1)}\|_F \right| \leq \epsilon$, where ϵ is the convergence parameter. Once the algorithm terminates, the vector of estimated delays, Dopplers, and channel coefficients are used to construct the estimated channel matrix using (11).

IV. Results and Discussions

In this section, we present the performance results for the proposed channel estimation algorithm. We also present the performance of the 1D off-grid SBL based algorithm in [9] for comparison. A DZT-OTFS system with $K = 16$, $L = 48$, carrier frequency $f_c = 3$ GHz, $B = 200$ kHz, and $T_{\text{s}} = \frac{1}{B} = 5$ μs is considered. The transmit and receive pulses are taken to be square-root raised cosine (SRRC) pulses (unless stated otherwise) with roll-off factor $\gamma = 0.5$. When $p(t)$ is SRRC pulse with roll-off factor γ, $g(t)$ is raised cosine pulse with roll-off factor γ, given by $g(t) = \frac{\sin(\pi t/T_{\text{s}})\cos(\gamma\pi t/T_{\text{s}})}{(\pi t/T_{\text{s}})(1-(2\gamma t/T_{\text{s}})^2)}$. A channel with $P = 4$, $\tau_{\max} = 4\Delta\tau$, and $\nu_{\max} = 3\Delta\nu$ is considered. $\tau_i \in \text{U}[0, \tau_{\max}]$ and $\nu_i \in \text{U}[-\nu_{\max}, \nu_{\max}]$, where U[.,.] denotes uniform distribution. The channel coefficients are considered to have an exponential power delay profile with $h_i \sim \mathcal{CN}(0, \sigma_i^2)$, where $\sigma_i^2 = \frac{e^{-0.1\alpha_i}}{\sum_i e^{-0.1\alpha_i}}$ [9]. The following algorithm parameters are used: $(k_{\text{tx}}, l_{\text{tx}}) = (K/2, L/2)$, $E_{\text{f}} = 1$, $P_{\max} = 15$, and $\Delta_\alpha = \Delta_\beta = 0.1$. QPSK modulation and minimum mean square error (MMSE) detection are used.

Choice of σ_{p}^2: Recall, $\sigma_{\text{p}}^2 + \sigma_{\text{d}}^2 = E_{\text{f}}$. Large σ_{p}^2 is good for channel estimation but bad for detection due to increased pilot interference. Likewise, large σ_{d}^2 is good for detection but bad

TABLE I
PER ITERATION COMPLEXITY IN SBL [9] AND PROPOSED ALGORITHMS

Operation	SBL algorithm [9]	Proposed algorithm
Complex multiplications	$M_T N_T M_\tau N_\nu(11M_\tau N_\nu + 2M_T N_T) + 2M_\tau N_\nu + 2(M_\tau N_\nu)^2(2 + M_T N_T) + M_T^3 N_T^3 + 2(\hat{P}^3 + \hat{P}^2)$	$3 + KL + \frac{KL}{2}\log_2(KL)(2 + \frac{1}{\Delta\alpha} + \frac{1}{\Delta\beta}) + K^2L^2(\frac{1}{\Delta\alpha} + \frac{1}{\Delta\beta})$
Complex additions	$M_T N_T M_\tau N_\nu(13M_\tau N_\nu + 2M_T N_T - 6) + M_T N_T - M_T^2 N_T^2 + 3M_\tau N_\nu + 2M_\tau^2 N_\nu^2 + 2(\hat{P}^2 - \hat{P})$	$\frac{3}{\Delta\alpha} + KL\log_2(KL)(2 + \frac{1}{\Delta\alpha} + \frac{1}{\Delta\beta}) + KL(KL-1)(\frac{1}{\Delta\alpha} + \frac{1}{\Delta\beta})$
Real multiplications	$M_T N_T + 3M_\tau N_\nu + 2$	$\frac{8KL}{\Delta\alpha}$
Real additions	$3M_\tau N_\nu + 3$	$2 + \frac{KL}{\Delta\alpha}$

for channel estimation. This performance trade-off is captured in Fig. 2 which shows BER plots as a function of $\sigma_{\rm p}^2$. It is seen that $\sigma_{\rm p}^2 = 0.2$ gives the minimum BER. Therefore, $\sigma_{\rm p}^2 = 0.2$ is used in all subsequent simulations.

Choice of ϵ: Choosing ϵ value is critical as it influences the number of paths picked up before the termination of the algorithm. A small ϵ can result in more paths being picked up, which may include noise being picked up as valid paths. A large ϵ can lead to fewer paths being picked up than the number of valid paths. The optimum ϵ depends on SNR. Lower the SNR, higher will be ϵ to avoid noise being picked up as valid paths. We have simulated the NMSE and BER performance, where NMSE is defined as $\frac{\|\mathbf{H}-\hat{\mathbf{H}}\|_F^2}{\|\mathbf{H}\|_F^2}$, and obtained the optimum ϵ for which the NMSE and BER are minimum. The optimum ϵ values obtained for different SNRs are given in (SNR in dB, ϵ) format as: $\{(0, 0.7), (5, 0.5), (10, 0.3), (15, 0.05), (20, 0.01), (25, 0.001\}$.

NMSE and BER performance: Figures 3 and 4 show the NMSE and BER performance of the proposed algorithm for SRRC pulse. Performance of the 1D off-grid SBL algorithm in [9] adapted to DZT-OTFS with SRRC pulse is also plotted. Performance with perfect channel state information (CSI) is also shown. From Fig. 3, it is seen that the NMSE performance of the proposed algorithm is better than that obtained using the 1D off-grid SBL algorithm by about 2 dB. This better channel estimation performance of the proposed algorithm translates into better BER performance. This can be seen in Fig. 4 where the performance of both algorithms are about the same up to 10 dB SNR, but beyond that the proposed algorithm performs better. The performance of the proposed algorithm for rectangular pulse ($p(t) = 1/\sqrt{T_{\rm s}}$ for $0 \le t \le T_{\rm s}$, and 0 otherwise) is also shown. It is seen that the performance with SRRC pulse is marginally better than with rectangular pulse. Both pulses perform close to their respective perfect CSI performance.

Complexity comparison: The number of complex and real multiplications and additions in one iteration of [9] and proposed algorithm for SRRC pulse is provided in Table I. The number of iterations in proposed algorithm is SNR dependent, and the maximum number of iterations is 15. The average number of iterations until convergence in [9] is 127. For the system parameters considered, the proposed algorithm requires a total of 3.58×10^8 operations. In [9], with $N = 16, M = 48, M_\tau = 9, N_\nu = 61, M_T = 7, N_T = 5, \hat{P} = 5$, the total number of operations is 3.54×10^{10}. Hence, the proposed algorithm is computationally more efficient and this has been witnessed in simulation run time as well (0.36 s run time for the proposed algorithm and 31.28 s for the algorithm in [9]).

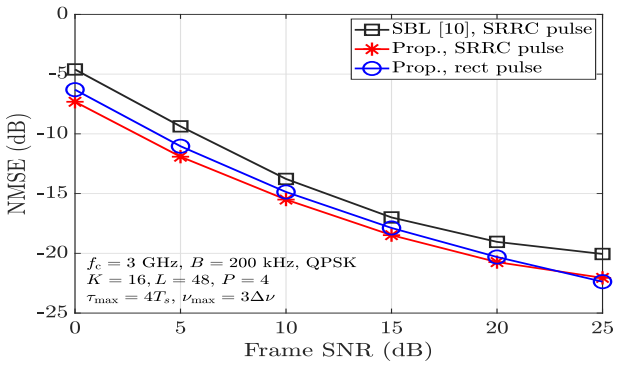

Fig. 3. NMSE performance comparison between proposed algorithm and 1D off-grid SBL estimation algorithm in [9].

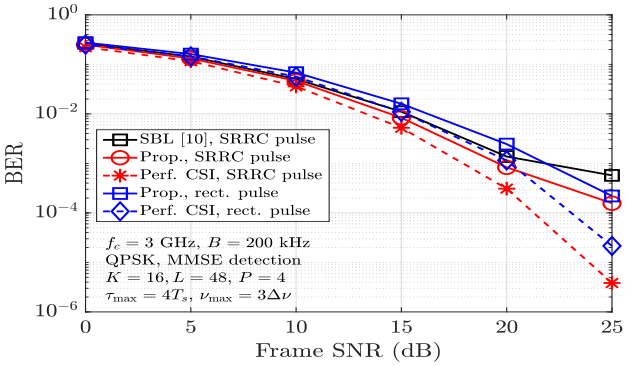

Fig. 4. BER performance comparison between proposed algorithm and 1D off-grid SBL estimation algorithm in [9].

REFERENCES

[1] Z. Wei et al., "Orthogonal time-frequency space modulation: a promising next-generation waveform," *IEEE Wireless Commun. Mag.*, vol. 28, no. 4, pp. 136-144, Aug. 2021.
[2] A. J. E. M. Janssen, "The Zak transform: a signal transform for sampled time-continuous signals," *Philips J. Res.*, 43, pp. 23-69, 1988.
[3] S. K. Mohammed, R. Hadani, A. Chockalingam, and R. Calderbank, "OTFS - a mathematical foundation for communication and radar sensing in the delay-Doppler domain," *IEEE BITS the Information Theory Magazine*, vol. 2, no. 2, pp. 36-55, Nov. 2022.
[4] S. K. Mohammed, R. Hadani, A. Chockalingam, and R. Calderbank, "OTFS - predictability in the delay-Doppler domain and its value to communication and radar sensing," available https://arxiv.org/abs/2302.08705.
[5] F. Lampel, A. Avarado, and F. M. J. Willems, "On OTFS using the discrete Zak transform," *IEEE ICC'2022 Workshops*, pp. 729-734, May 2022.
[6] V. Yogesh, V. Bhat, S. R. Mattu, and A. Chockalingam, "On the bit error performance of OTFS modulation using discrete Zak transform," *IEEE ICC'2023*, pp. 741-746, May-Jun. 2023.
[7] I. A. Khan and S. K. Mohammed, "A low-complexity OTFS channel estimation method for fractional delay-Doppler scenarios," *IEEE Wireless Commun. Lett.*, vol. 12, no. 9, pp. 1484-1488, Sep. 2023.
[8] R. Horn and C. Johnson, *Matrix Analysis*, Cambridge Univ. Press, 2013.
[9] Z. Wei, W. Yuan, S. Li, J. Yuan, and D. W. K. Ng, "Off-grid channel estimation with sparse Bayesian learning for OTFS systems," *IEEE Trans. Wireless Commun.*, vol. 21, no. 9, pp. 7407-7426, Mar. 2022.
[10] H. Bolcskei and F. Hlawatsch, "Discrete Zak transforms, polyphase transforms, and applications," *IEEE Trans. Signal Process.*, vol. 45, no. 4, pp. 851-866, Apr. 1997.